Molecular Biology of the Cell
Vol. 10, 2377–2391, July 1999

Yeast Dam1p Is Required to Maintain Spindle Integrity during Mitosis and Interacts with the Mps1p Kinase

Michele H. Jones, Jeffrey B. Bachant,* Andrea R. Castillo, Thomas H. Giddings, Jr., and Mark Winey†

Department of Molecular, Cellular, and Developmental Biology, University of Colorado–Boulder, Boulder Colorado 80309-0347

Submitted December 28, 1998; Accepted April 26, 1999
Monitoring Editor: Tim Stearns

We have identified a mutant allele of the *DAM1* gene in a screen for mutations that are lethal in combination with the *mps1-1* mutation. *MPS1* encodes an essential protein kinase that is required for duplication of the spindle pole body and for the spindle assembly checkpoint. Mutations in six different genes were found to be lethal in combination with *mps1-1*, of which only *DAM1* was novel. The remaining genes encode a checkpoint protein, Bub1p, and four chaperone proteins, Sti1p, Hsc82p, Cdc37p, and Ydj1p. *DAM1* is an essential gene that encodes a protein recently described as a member of a microtubule binding complex. We report here that cells harboring the *dam1-1* mutation fail to maintain spindle integrity during anaphase at the restrictive temperature. Consistent with this phenotype, *DAM1* displays genetic interactions with *STU1*, *CIN8*, and *KAR3*, genes encoding proteins involved in spindle function. We have observed that a Dam1p-Myc fusion protein expressed at endogenous levels and localized by immunofluorescence microscopy, appears to be evenly distributed along short mitotic spindles but is found at the spindle poles at later times in mitosis.

INTRODUCTION

The mitotic spindle serves to segregate replicated chromosomes to progeny cells during cell division. This sophisticated microtubule-based structure is organized from two spindle poles on opposing sides of the nucleus that contain centrosomes or equivalent organelles (Kellogg *et al.*, 1994). In the budding yeast *Saccharomyces cerevisiae*, the centrosome-equivalent organelle is the spindle pole body (SPB) (Botstein *et al.*, 1997; Winsor and Schiebel, 1997). The SPB is a multilayered organelle, which remains embedded in the nuclear envelope throughout the yeast cell cycle (Byers and Goetsch, 1975). The SPB contains γ-tubulin (the product of the *TUB4* gene) and the associated Spc97p and Spc98p, all of which are required for microtubule nucleation (Knop *et al.*, 1997; Knop and Schiebel, 1997, 1998; Sundberg and Davis, 1997), a key function of the SPB. Centrosome duplication is a critical cell cycle–regulated event required for the formation of a bipolar spindle. In budding yeast, the SPB is duplicated late in the G1 phase of the cell cycle (Byers and Goetsch, 1974, 1975). The duplication pathway has been described morphologically, and several genes required for the process have been identified by mutation (Winey and Byers, 1993; Botstein *et al.*, 1997). Among the genes required for SPB duplication is *MPS1* (for monopolar spindle), which encodes an essential protein kinase (Winey *et al.*, 1991; Lauze *et al.*, 1995). Analysis of strains containing different mutant alleles of *MPS1* reveals two distinct SPB duplication defects, suggesting that Mps1p has at least two distinct functions in SPB duplication (Schutz and Winey, 1998).

After SPB duplication, the SPBs separate as the mitotic spindle is assembled. Later in the cell cycle, the

* Present address: Department of Biochemistry, Baylor College of Medicine, 1 Baylor Plaza, Houston, TX 77030.
† Corresponding author. E-mail address: Mark.Winey@Colorado.edu.

Abbreviations used: 5-FOA, 5-fluoroorotic acid; GFP, green fluorescent protein; SPB, spindle pole body.

© 1999 by The American Society for Cell Biology

spindle segregates chromosomes by both anaphase A and anaphase B movements (Winey *et al*., 1995; Straight *et al*., 1997). A number of proteins are required for these processes, including several that are localized to the spindle and spindle pole (for review, see (Hoyt and Geiser, 1996; Botstein *et al*., 1997). These include a variety of microtubule-based molecular motors, both kinesin-related proteins (Cin8p, Kar3p, and Kip1p) and dynein (Dhc1p). There are also nonmotor spindle components such as Stu1p, Ase1p, and Duo1p that are required for spindle function. Finally, components of the kinetochore, which connect the chromosomes to the spindle, contribute to spindle formation and integrity (e.g., Mif2p; Brown *et al*., 1993). Extensive genetic interactions have been detected between alleles of the various genes required for spindle assembly and function.

The assembly of the mitotic spindle and the execution of mitosis are both under strict cell cycle control. Both SPB duplication and the separation of the SPBs to form the spindle require *CDC28/CLN* activity (Winey and Byers, 1993; Winsor and Schiebel, 1997). The onset of anaphase requires the degradation of the Esp1p inhibitor Pds1p by the anaphase-promoting complex (Cohen-Fix *et al*., 1996), and exit from mitosis requires complete inactivation of *CDC28/CLBs* as well as the degradation of the spindle component Ase1p (Juang *et al*., 1997). These controls are executed during each round of cell division and serve to coordinate activities of the mitotic spindle with other cell cycle events. A distinct set of cell cycle controls, termed checkpoint pathways, are inducible and function to block mitotic progression when the DNA or the spindle is damaged or when a prerequisite event has not occurred (Elledge, 1996). For example, the spindle assembly checkpoint pathway delays the onset of anaphase when spindle function is compromised by microtubule-depolymerizing agents or by mutations that affect assembly or integrity of the mitotic spindle (Rudner and Murray, 1996; Wells and Murray, 1996). In addition to its role in SPB duplication, Mps1p kinase is also required for activation of the spindle assembly checkpoint, most likely through phosphorylation of Mad1p, another constituent of this signaling pathway (Hardwick *et al*., 1996; Weiss and Winey, 1996). Thus far, all conditional mutations in *MPS1* lie in the kinase domain, and all affect both the SPB duplication and the checkpoint functions (Schutz and Winey, 1998).

We have endeavored to understand how Mps1p functions in its dual roles by identifying factors with which it interacts, either genetically or physically. We previously reported that *MPS1* and the molecular chaperone gene *CDC37* show a variety of genetic interactions and that Mps1p requires the Cdc37p for kinase activity (Schutz *et al*., 1997). *MPS1* also shows genetic interactions with *CIN8*, a spindle motor gene, suggesting a potential role for Mps1p at the spindle that may be distinct from its functions in SPB duplication and spindle checkpoint activation (Geiser *et al*., 1997). Finally, Mps1p has been found by two-hybrid and coimmunoprecipitation experiments to bind Mob1p (Luca and Winey, 1998). Mob1p is required for the completion of mitosis and the maintenance of ploidy; the latter function requires Mps1p activity and may be related to the role of Mps1p in SPB duplication.

Here we report that six genes were identified by mutations that caused inviability in combination with the *mps1-1* mutation. One of these genes encodes Bub1p, a kinase that, like Mps1p, is required for the spindle assembly checkpoint (Hoyt *et al*., 1991; Roberts *et al*., 1994). Several of the other genes encode molecular chaperones, suggesting a single kinase may require several different chaperones for activity. Last, we identified a novel gene that encodes an essential coiled-coil protein. This gene, *DAM1*, was independently identified in a screen for proteins that interact with a spindle-associated protein, Duo1p (Hofmann *et al*., 1998; also see Figure 6), and Dam1p has been shown to bind microtubules in vitro. Our findings indicate that Dam1p is required for spindle integrity during anaphase B elongation, and that the protein is localized to short spindles and spindle poles during the cell cycle. The fact that a mutation in *MPS1* exhibits a genetic interaction with an allele of *DAM1* reinforces the idea that Mps1p may have essential roles in both SPB and spindle function.

MATERIALS AND METHODS

Yeast and Escherichia coli Culture and Genetic Techniques

The yeast strains used in this study are listed in Table 1. Yeast growth conditions (including media) and yeast genetic techniques were as described (Guthrie and Fink, 1991). Most strains derive from the S288c background. The cell synchronization experiments were performed by treating cultures (0.4 OD units) with 10 μM α-factor (US Biological, Swampscott, MA) for ~2 h, washing two times, and then resuspending in warmed media. Percentage of large budded cells was measured by counting those cells with a bud size greater than half the size of the mother cell. Depolymerizaton of microtubules was performed as described (Hardwick *et al*., 1996). Samples were prepared after 3 h in media containing benomyl (DuPont, Wilmington, DE) and nocodazole (US Biological) for flow cytometry (60% large budded; our unpublished results) and immunofluorescence as described below.

Synthetic Lethal Screen and Gene Cloning

Mutant strains that require *MPS1* at the normally permissive (ambient, ~23°C) *mps1-1* temperature (*mps1-1* enhancer [*moe*]) were derived from three strains, 12a, 15b, and 7d (Table 1). These strains contain the *mps1-1 ts* allele and a mutant alleles of *ade2, ade3*, and *ura3*. They harbor a plasmid with the yeast markers *ADE3* and *URA3* and a wild-type copy of *MPS1*. The *ADE3* and *URA3* yeast markers allowed us to assess the requirement of these strains for the wild-type copy of *MPS1* using the adenine red–white sectoring assay (Bender and Pringle, 1991) and resistance to 5-fluoroorotic

Table 1. Yeast strains

Strain	Genotype
7d	*MAT**a**, mps1-1, ade2, ade3, his3Δ200, leu2-3,112, ura3-52, lys2-801 (MPS1-URA3,ADE3,CEN)*
12a	*MATα, mps1-1, ade2, ade3, his3Δ200, leu2-3,112, ura3-52, lys2-801 (MPS1-URA3,ADE3,CEN)*
15b	*MATα, mps1-1, ade2, ade3, his3Δ200, leu2-3,112, ura3-52, lys2-801 (MPS1-URA3,ADE3,CEN)*
12a30-69	*MATα, moe1, mps1-1, ade2, ade3, his3Δ200, leu2-3,112, ura3-52, lys2-801 (MPS1-URA3,ADE3,CEN)*
12a30-70	*MATα, moe2, mps1-1, ade2, ade3, his3Δ200, leu2-3,112, ura3-52, lys2-801 (MPS1-URA3,ADE3,CEN)*
15b20-11	*MATα, moe2, mps1-1, ade2, ade3, his3Δ200, leu2-3,112, ura3-52, lys2-801 (MPS1-URA3,ADE3,CEN)*
15b45-5	*MATα, moe7, mps1-1, ade2, ade3, his3Δ200, leu2-3,112, ura3-52, lys2-801(MPS1-URA3,ADE3,CEN)*
15b45-68	*MATα, moe13, mps1-1, ade2, ade3, his3Δ200, leu2-3,112, ura3-52, lys2-801 (MPS1-URA3,ADE3,CEN)*
15b45-188	*MATα, moe21, mps1-1, ade2, ade3, his3Δ200, leu2-3,112, ura3-52, lys2-801 (MPS1-URA3,ADE3,CEN)*
15b45-279	*MATα, moe27, mps1-1, ade2, ade3, his3Δ200, leu2-3,112, ura3-52, lys2-801 (MPS1-URA3,ADE3,CEN)*
15b45-341	*MATα, moe34, mps1-1, ade2, ade3, his3Δ200, leu2-3,112, ura3-52, lys2-801 (MPS1-URA3,ADE3,CEN)*
15b45-69	*MATα, moe14(1), mps1-1, ade2, ade3, his3Δ200, leu2-3,112, ura3-52, lys2-801 (MPS1-URA3,ADE3,CEN)*
15b45-248	*MATα, moe25, mps1-1, ade2, ade3, his3Δ200, leu2-3,112, ura3-52, lys2-801 (MPS1-URA3,ADE3,CEN)*
15b45-298	*MATα, moe29, mps1-1, ade2, ade3, his3Δ200, leu2-3,112, ura3-52, lys2-801 (MPS1-URA3,ADE3,CEN)*
15b45-69	*MATα, moe14(2), mps1-1, ade2, ade3, his3Δ200, leu2-3,112, ura3-52, lys2-801 (MPS1-URA3,ADE3,CEN)*
15b30-4	*MATα, moe4, mps1-1, ade2, ade3, his3Δ200, leu2-3,112, ura3-52, lys2-801 (MPS1-URA3,ADE3,CEN)*
15b45-59	*MATα, moe12, mps1-1, ade2, ade3, his3Δ200, leu2-3,112, ura3-52, lys2-801 (MPS1-URA3,ADE3,CEN)*
15b45-156	*MATα, moe15, mps1-1, ade2, ade3, his3Δ200, leu2-3,112, ura3-52, lys2-801 (MPS1-URA3,ADE3,CEN)*
15b45-240	*MATα, moe24, mps1-1, ade2, ade3, his3Δ200, leu2-3,112, ura3-52, lys2-801 (MPS1-URA3,ADE3,CEN)*
15b45-262	*MATα, moe26, mps1-1, ade2, ade3, his3Δ200, leu2-3,112, ura3-52, lys2-801 (MPS1-URA3,ADE3,CEN)*
15b45-295	*MATα, moe28, mps1-1, ade2, ade3, his3Δ200, leu2-3,112, ura3-52, lys2-801 (MPS1-URA3,ADE3,CEN)*
15b45-335	*MATα, moe33, mps1-1, ade2, ade3, his3Δ200, leu2-3,112, ura3-52, lys2-801 (MPS1-URA3,ADE3,CEN)*
15b45-350	*MATα, moe35, mps1-1, ade2, ade3, his3Δ200, leu2-3,112, ura3-52, lys2-801 (MPS1-URA3,ADE3,CEN)*
7d45-1	*MAT**a**, moe37, mps1-1, ade2, ade3, his3Δ200, leu2-3,112, ura3-52, lys2-801, (MPS1-URA3,ADE3,CEN)*
WX241-20c(295)	*MAT**a**, mps1-1, ura3-52, his3Δ200*
DB8WX257-15c[a]	*MAT**a**, mps1Δ::HIS3, ura3-52, leu2-3,112, trp1Δ1, his3Δ200 (MPS1-URA3,CEN)*
WX257-17c(371)	*MAT**a**, ura3-52, leu2-3,112, trp1Δ1, his3Δ200*
D8bX5cA(375)[a]	*MAT**a**/MATα, ura3-52/ura3-52, leu2-3,112/leu2-3,112, trp1Δ1/trp1Δ1, his3Δ200/his3Δ200*
MJYM14-9b(889)	*MAT**a**, dam1-1, ura3-52, leu2-3,112, trp1Δ1, his3Δ200*
moe1b/1d (908)	*MAT**a**/MATα, dam1-1/dam1-1, ura3-52/ura3-52, leu2-3,112/leu2-3,112, TRP/trp1Δ1, HIS3/his3Δ200*
MHJ19-5b(1325)	*MAT**a**, dam1-1, mad1Δ2::URA3, ura3-52, leu2-3,112, his3Δ200, ade2-1*
MHJ39-8c(1491)	*MAT**a**, dam1-1, mad2Δ::URA3, ura3-52, leu2-3,112, trp1Δ1*
MHJ39-8c(1495)	*MAT**a**, dam1-1, mad3Δ::URA3, ura3-52, leu2-3,112, trp1Δ1, his3Δ200, ade2-1, can1-100*
MHJ22-1b(1341)	*MAT**a**, dam1-1, cin8Δ::HIS3, ura3-52, leu2-3,112, trp1Δ1, his3Δ200, lys2-801, cyh2^R, can1-100 (DAM1-URA3-CEN)*
MHJ38-2a(1485)	*MATα, dam1-1, kar3Δ::LEU2, ura3-52, leu2-3,112, his3Δ200 (KAR3-URA3-2μ)*
MHJ37-8b(1547)	*MAT**a**, DAM1-MYC::HIS3, SPC42-GFP::TRP, SPC42Δ::LEU2, ura3-52, leu2-3,112, his3Δ200, trp1-1*
8bX15a-1(1549)	*MAT**a**/MATα, DAM1-MYC::HIS3/DAM1-MYC::HIS3, SPC42-GFP::TRP/SPC42-GFP::TRP, SPC42Δ::LEU2/SPC42Δ::LEU2, ura3-52/ura3-52, leu2-3,112/leu2-3,112, his3Δ200/his3Δ200, trp1-1/trp1-1*
MHJMM (1345)	*MAT**a**/MATα, DAM1-MYC::HIS3/DAM1-MYC::HIS3, ura3-52/ura3-52, leu2-3,112/leu2-3,112, his3Δ200/his3Δ200, TRP/trp1Δ1*
MHJΔDAM1 (950)	*MAT**a**/MATα, dam1Δ::HIS3/DAM1, ura3-52/ura3-52, leu2-3,112/leu2-3,112, his3Δ200/his3Δ200, trp1Δ1/trp1Δ1,*
WX257-14c(372)	*MAT**a**, ura3-52, leu2-3,112, trp1Δ1, his3Δ200*

All strains from this study except [a]Lauze *et al.* (1995).

acid (5-FOA, a suicide substrate for strains with the *URA3* gene product; Boeke *et al.*, 1987). Strains 12a, 15b, and 7d were mutagenized using methane sulfonic acid ethyl ester (Sigma, St. Louis, MO) to between 40 and 50% viability (Guthrie and Fink, 1991). Mutagenized cultures were plated on rich (YPD) media, and 93,000 colonies were screened for a solid red colony phenotype that would indicate the strain was unable to lose the wild-type copy of *MPS1*. Seven hundred eighty-seven (0.8%) nonsectoring colonies were further analyzed for their requirement for wild-type *MPS1* by checking them for 5-FOA sensitivity. Twenty-two of these strains were consistently nonsectoring and 5-FOA resistant. To demonstrate the above phenotypes were due to the requirement of these strains for *MSP1*, a *LYS2*-based plasmid containing *MPS1* was transformed into the strains, and all 22 were subsequently shown to sector and be 5-FOA resistant.

To distinguish between a bona fide *moe* mutation and the creation of an *mps1* chromosomal null within these strains, they were crossed to an *mps1*Δ strain (DB8WX257-5C; Table 1) supported by a *URA3*-based plasmid harboring a wild-type copy of *MPS1*. The resulting diploids were struck to 5-FOA-containing medium at an *mps1-1* permissive temperature to determine whether they required the wild-type copy of *MPS1*. Nine of the diploids from these crosses were 5-FOA sensitive, indicating that an additional mutation within *mps1-1* had generated a chromosomal null; these *mps1*Δ strains behave phenotypically as *moe* strains by being nonsectoring and 5-FOA sensitive.

The nature of the *moe* mutations was assessed by crossing the strains to a *mps1-1* strain (WX241-20c; Table 1). All 13 of the *mps1-1* homozygous, *moe* heterozygous diploids were 5-FOA resistant, suggesting that the *moe* mutations were recessive. To determine whether the synthetic lethal phenotype in the original *moe* strains was due to a mutation in a single gene, these diploids were sporulated, and resulting tetrads were dissected. Spores were analyzed for viability on 5-FOA medium. For all but two of the 13 *moe* strains,

Table 2. *moe* mutations

Complementation group	Members	Previously identified genes[a]
I	*dam1-1*	YGR113W/*DAM1*
II	*moe2*	*YDJ1*
III	*moe3, moe7, moe13*	*CDC37*
IV	*moe21, moe27, moe34*	*STI1*
V	*moe14(1), moe25*	*HSC82*
VI	*moe29*	*BUB1*
VII	*moe14(2)*	Not yet identified
VIII	*moe4, moe12, moe15, moe24, moe26, moe28, moe33, moe35, moe37*	*mps1* null alleles

[a] See text for literature citations.

the tetrads segregated 2:2 for synthetic lethality, suggesting that the *moe* phenotype was due to a mutation in a single gene.

Complementation analyses were carried out to determine the number of genes represented by the 13 remaining *moe* strains. Because many of the *moe* strains identified were of the same mating type, the strains were crossed to a *mps1-1* strain (WX241-20c; Table 1) to obtain the mutation in the opposite mating type. Spores resulting from this cross that were 5-FOA sensitive, and hence contained both the *mps1-1* and *moe* mutations, were analyzed for their mating type. Both *MAT***a** and *MAT*α *moe* mutant strains were intercrossed, and resulting diploids were replica plated to 5-FOA medium to determine whether the *moe* strains could complement one another. This analysis revealed seven genes, six of which are known (Table 2).

Complementation groups I, II, and III (Table 2) were cloned by complementation of the *ts* phenotype of the respective mutation upon transformation of these strains with a *LEU*-based centromeric yeast genomic library (a gift from C. Connelly and P. Heiter, University of British Columbia, Vancouver, Canada) and found to be the known genes, *DAM1*, *YDJ1*, and *CDC37*. To ensure that we had cloned the gene responsible for the *mps1-1* synthetic lethal phenotype, we determined that the corresponding null strain (see below) did not complement the original *ts* strain. Genes representing complementation groups IV, V, and VI were cloned by restoration of their sectoring and 5-FOA resistance phenotypes upon transformation with the *LEU*-based centromeric yeast genomic library. The gene corresponding to *moe14*[2] is being isolated (VII; Table 2).

DAM1 Plasmids, DAM1 Gene Disruption, and myc-DAM1

Multicopy plasmids containing the *DAM1* gene were constructed by inserting a 5-kb *Xba*I–*Sal*I fragment containing the *DAM1* gene into plasmids pRS424 and pRS426 (Sikorski and Hieter, 1989) cut with *Spe*1–*Sal*I. A precise deletion of the *DAM1* gene and replacement with the *HIS3* gene was done by one-step gene replacement (Baudin *et al*., 1993) in wild-type diploid strain 375 (Table 1) with a PCR product containing 42 bp of *DAM1* gene flanking sequences on either side of the *HIS3* gene. Histidine prototrophs were selected, and correct integration was confirmed using PCR amplification (Luca and Winey, 1998). A haploid strain containing the *DAM1* null allele was obtained by sporulation and dissection. Oligonucleotide primers were purchased from Life Technologies (Gaithersburg, MD). The strain containing the *myc-DAM1* fusion gene was constructed by transformation of wild-type strain with a PCR product containing the following sequence: from −80 bp to the stop codon of the *DAM1* gene, a triple repeat of the myc epitope (Kolodziej and Young, 1991), the *HIS3* gene, and the 3′ untranslated region of *DAM1* from +76 to +148. Histidine prototrophs were selected and analyzed by PCR amplification to confirm correct integration and by Western analysis to confirm protein expression as described (Luca and Winey, 1998), using a mouse anti-myc 1° antibody (1:1000; Santa Cruz Biotechnology, Santa Cruz, CA) and sheep anti-mouse 2° antibody conjugated to HRP (1:20,000; Amersham Pharmacia Biotech, Piscataway, NJ).

Cytological Techniques

Flow cytometric analysis of cells was performed as described using the DNA stain propidium iodide (Sigma) (Hutter and Eipel, 1979). Samples were analyzed on a Becton Dickinson (Mountain View, CA) FACScan flow cytometer using CELL QUEST software to obtain and analyze data (BDIS, San Jose, CA).

Fixation techniques and immunofluorescence of microtubules using 1° monoclonal antibody YOL1/34 and 2° anti-rat conjugated to FITC or Texas Red (Accurate Chemical and Scientific, Westbury, NY) and visualization of DNA using DAPI stain were performed as described (Pringle *et al*., 1991). The techniques used to visualize Dam1p-myc involved either the technique described for microtubules or a formaldehyde–methanol–acetone technique as described (Chial *et al*., 1998), in the second case, using a mouse anti-myc 1° antibody (1:300; Santa Cruz Biotechnology) and a sheep anti-mouse 2° antibody conjugated to Texas Red or FITC (1:800; Jackson ImmunoResearch, West Grove, PA). Standard fluorescence microscopy was carried out using either a Zeiss (Thornwood, NY) fluorescence microscope with an Empix charge-coupled device camera and Metamorph Software (Universal Imaging, Westchester, PA) or a Leica DMRXA/RF4/V automated microscope with a Cooke SensiCam digital camera and Slidebook software (Intelligent Imaging Innovations, Denver, CO). Yeast cells were prepared for thin sectioning as described by (Byers and Goetsch, 1991). Serial sections were viewed on a Philips CM10 electron microscope (Philips Electronic Instruments, Mahwah, NJ).

RESULTS

Synthetic Lethal Screen

A screen for mutations that are lethal in combination with the *mps1-1* mutation was conducted to identify genes whose products interact with the Mps1p kinase (*moe* = *m*ps *o*ne *e*nhancer). At restrictive temperatures the *mps1-1* allele is defective for SPB duplication (Winey *et al*., 1991) and, subsequently, in the spindle assembly checkpoint (Weiss and Winey, 1996). The mutation in this allele lies in the kinase domain and greatly decreases protein kinase activity in vitro (Schutz and Winey, 1998). Mutations lethal in combination with *mps1-1* at its permissive temperature were initially identified in a plasmid-sectoring assay based on the adenine biosynthetic pathway (Bender and Pringle, 1991). After mutagenisis (see MATERIALS AND METHODS) nonsectoring solid red colonies were selected as candidates because they appeared to require the *MPS1*-containing plasmid. The inability of the solid red colonies to lose the wild-type copy of *MPS1* was confirmed by their failure to grow on 5-FOA medium that selects against cells harboring the plasmid-borne *URA3* gene (Boeke *et al*., 1987). Finally, to demonstrate that the nonsectoring and 5-FOA sensitivity phenotypes were due to the strains' require-

ment for the plasmid-borne wild-type *MPS1*, a second *MPS1*-containing plasmid was transformed into candidate strains, and the transformed strains were shown to sector and grow on 5-FOA medium. Twenty-two independently isolated strains were identified in which colonies both fail to sector and fail to grow on 5-FOA medium, but in which both phenotypes were restored when another *MPS1* plasmid was introduced into the strain.

Genetic analysis of the 22 original isolates involved eliminating chromosomal null alleles of *MPS1* (nine were recovered; see MATERIALS AND METHODS), screening for additional phenotypes, and segregation and complementation analysis. For all but 2 of the 13 remaining strains, the synthetic lethality segregated as a single mutation. One of these two was not studied further, because the synthetic lethal phenotype was due to mutations in more than one gene. However, for the second aberrantly segregating strain two separable mutations were identified, each of which was lethal in combination with *mps1-1*. Three of the 13 strains were found to have temperature-sensitive growth defects. The *ts* phenotype cosegregated with the synthetic lethality in all three strains. Complementation analysis (Table 2) revealed that each of the synthetic lethal mutations that give temperature-sensitive growth defects defines separate complementation groups and that two of these groups each contain other nonconditional synthetic lethal alleles. The remaining nonconditional synthetic lethal mutations identified four complementation groups, two with multiple members (Table 2).

Identification of the Genes

We have previously reported alleles of the yeast *CDC37* gene, which encodes a molecular chaperone, that are lethal in combination with *mps1-1* (Schutz *et al.*, 1997). We tested to see whether any of the seven complementation groups of synthetic lethal mutations could be complemented by *CDC37*. One group (III; Table 2) consists of both conditional and nonconditional alleles of *CDC37*. Five of the six remaining genes were identified by complementation using a yeast genomic library (see MATERIALS AND METHODS). Consistent with our previous findings that the Mps1p kinase requires chaperone function for its activity, three of the genes identified, *HSC82, YDJ1*, and *STI1* (V, II, and IV; Table 2), encode chaperonins. *HSC82* encodes one of the two *S. cerevisiae* Hsp90 proteins that exhibit substrate specificity for kinases (Pratt, 1992; Jakob and Buchner, 1994; Nathan and Lindquist, 1995). *STI1* encodes an Hsp70p of the Ssa subclass that has been found in a complex with Hsp90p (Chang and Lindquist, 1994). The third chaperone identified in this screen, Ydj1p, encodes a dnaJ homologue that has been shown to interact with and regulate the Ssa subclass of Hsp70s (Cyr *et al.*, 1992; Cyr, 1995; Cyr and Douglas, 1994). The strain that contained two mutations that were synthetically lethal with *mps1-1* had a mutation in *HSC82* and another as yet unidentified locus. Interestingly, an allele of the *BUB1* gene that encodes another protein kinase involved in the spindle assembly checkpoint was identified in the screen (VI; Table 2; Roberts *et al.*, 1994)). This allele of *BUB1*, called *bub1-656*, behaved similarly to previously identified *bub1* alleles (Hoyt *et al.*, 1991), in that it exhibited slow growth and benomyl sensitivity, suggesting that the checkpoint activity of *bub1-656* was compromised (our unpublished observation).

A conditional allele representing the final complementation group (I; Table 2) was rescued at the nonpermissive temperature by the uncharacterized YGR113W gene on chromosome VII. We constructed a null allele of this gene by exact gene replacement (see MATERIALS AND METHODS) and found that the gene is essential for viability. This gene, named *DAM1* (for Duo1p and Mps1p Interactor) has been independently identified in a screen for proteins that interact with a spindle-associated protein, Duo1p. Dam1p has also been shown to localize to the spindle when overexpressed and to bind microtubules in vitro (Hofmann *et al.*, 1998).

dam1-1 Strains Fail in Mitosis

We examined cells containing the *ts dam1-1* mutation (908; Table 1) at the nonpermissive temperature to understand more about the role of Dam1p in the cell. After 2.5 h at the nonpermissive temperature (37°C), a significant number of *dam1-1* cells arrest with large buds, as determined by budding index (47%; n = 400 cells), and with 2C DNA content as determined by flow cytometry (Figure 1A). The chromatin in these cells, as visualized by DAPI staining, is separated into two masses of approximately equal staining intensity, indicating that the cells have begun anaphase elongation of the spindle (Figure 1B, DAPI). In anaphase, *dam1-1* cells at the permissive temperature (Figure 1B, 25°C, α-Tubulin) and wild-type cells (our unpublished observation) contain mitotic spindles with interdigitated microtubules from each SPB that appear as a solid bar of microtubules between and overlapping the DAPI staining region. Strikingly, this structure is absent in *dam1-1* strains incubated at the nonpermissive temperature (Figure 1B, 37°C, α-Tubulin); instead, these cells contain two distinct microtubule-staining regions that appear to be the result of loss of integrity in the mitotic spindle. This "broken spindle" phenotype was confirmed by electron microscopic examination of the spindles in these cells. The cells were found to contain two SPBs, each with a distinct array of nuclear mictrotubules, but these microtubules are not interconnected as in a normal spindle (Figure 2 and

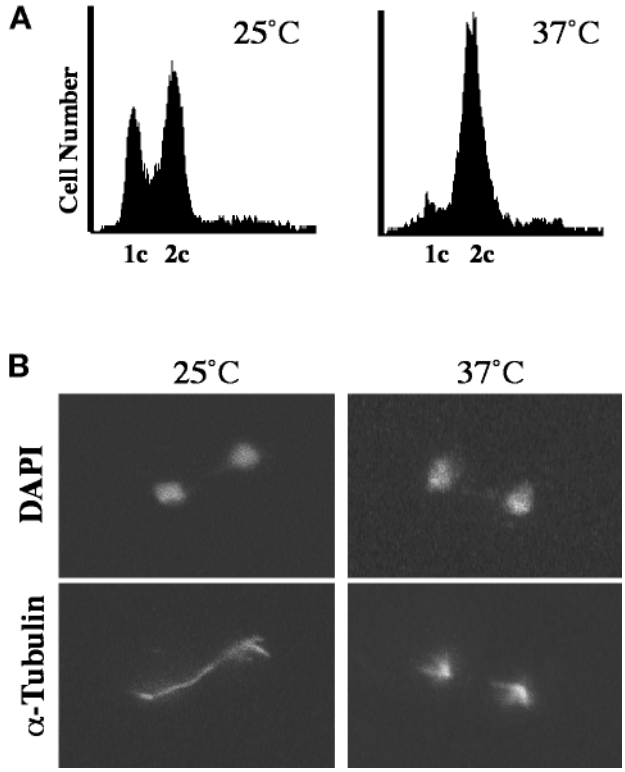

Figure 1. Characterization of the asynchronously growing diploid *dam1-1* strain at the permissive temperature (25°C) and after shift to the nonpermissive (37°C) temperature for 2.5 h. (A) Flow cytometric analysis to measure DNA content. 1C and 2C, DNA content (propidium iodide fluorescence) before and after DNA replication, respectively. Each histogram represents 5000 cells. (B) Immunofluorescence staining of DNA (DAPI) and tubulin (α-Tubulin) in cells grown at 25 and 37°C, as described in MATERIALS AND METHODS.

adjoining serial sections; our unpublished observation; see legend for quantitation). Consistent with these mitotic abnormalities, a significant loss of viability (>66% lethality upon return to the permissive temperature after 2.5 h at the nonpermissive temperature) was observed in *dam1-1* cells.

We examined *dam1-1* cells proceeding synchronously through the cell cycle at the nonpermissive temperature to determine the timing of development of the defective spindle phenotype. Wild-type and *dam1-1* strains (372 and 889; Table 1) were arrested in the G1 phase of the cell cycle at permissive temperature by treatment with α-factor and then released from this G1 arrest at the nonpermissive temperature (see MATERIALS AND METHODS). Cell cycle progression was monitored over time by quantitating the number of large-budded cells (%LB) and quantitating DNA content in the population of cells (Figure 3A). The mitotic spindles in these cells were monitored by immunofluorescence staining of microtubules (Figure 3B, α-Tubulin), and the DNA was detected by DAPI staining (Figure 3B, DAPI). Early mitotic spindles, before visible separation of the chromatin, appear to be similar in wild-type and *dam1-1* cells (Figure 3B, a). However, as cells proceed with anaphase elongation of the spindle (Figure 3B, b and c), the spindle remains intact in wild-type cells but breaks in *dam1-1* cells, yielding two distinct microtubule-staining arrays and partially separated chromatin. After 3.3 h at the nonpermissive temperature, 78% of *dam1-1* cells are large-budded, the majority containing defective spindles (see quantitation in figure legend). Additional experiments were conducted to determine the fate of these cells by monitoring the budding index of wild-type and *dam1-1* cells up to 6 h after release into the nonpermissive temperature (Figure 4). Although both strains start with a large percentage of unbudded cells because of treatment with α-factor, wild-type cells show a second increase in unbudded cells after 4 h, presumably because of normal cytokinesis to complete the cell cycle. In contrast, no unbudded cell population reappears in *dam1-1* cells over the course of the experiment; instead an increase in large and multibudded cells is observed at 4 h. The population of multibudded cells increases further after 6 hours, consistent with the idea that *dam1-1* cells do not undergo cytokinesis. Taken together, these results suggest a direct role for Dam1p during anaphase spindle elongation and another role, possibly indirect, during cytokinesis.

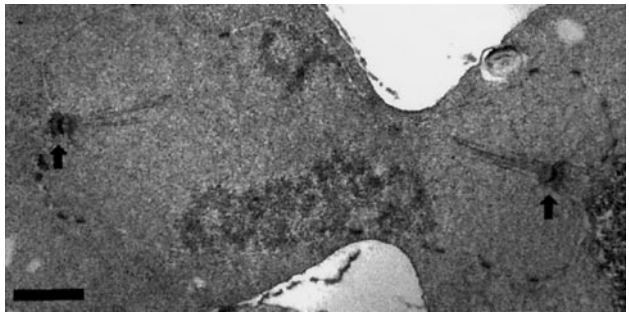

Figure 2. Electron micrograph of the asynchronously growing diploid *dam1-1* strain after shift to the nonpermissive (37°C) temperature for 2.5 h. Arrows denote spindle pole bodies. Bar, 0.5 μm. Of spindles examined from 13 large-budded cells, 11 were discontinuous as shown here, and 2 appeared normal.

dam1-1 Strains Do Not Constitutively Require the Spindle Assembly Checkpoint but Do Require Mad1p to Accumulate Mitotic Cells at the Nonpermissive Temperature

As described, *mps1-1* strains show documented defects both in SPB duplication and in the spindle assembly checkpoint pathway. The failure of the mitotic spindle in *dam1-1* strains suggested that the genetic interaction between *MPS1* and *DAM1* might reflect Mps1p's role in the checkpoint, i.e., that the normally

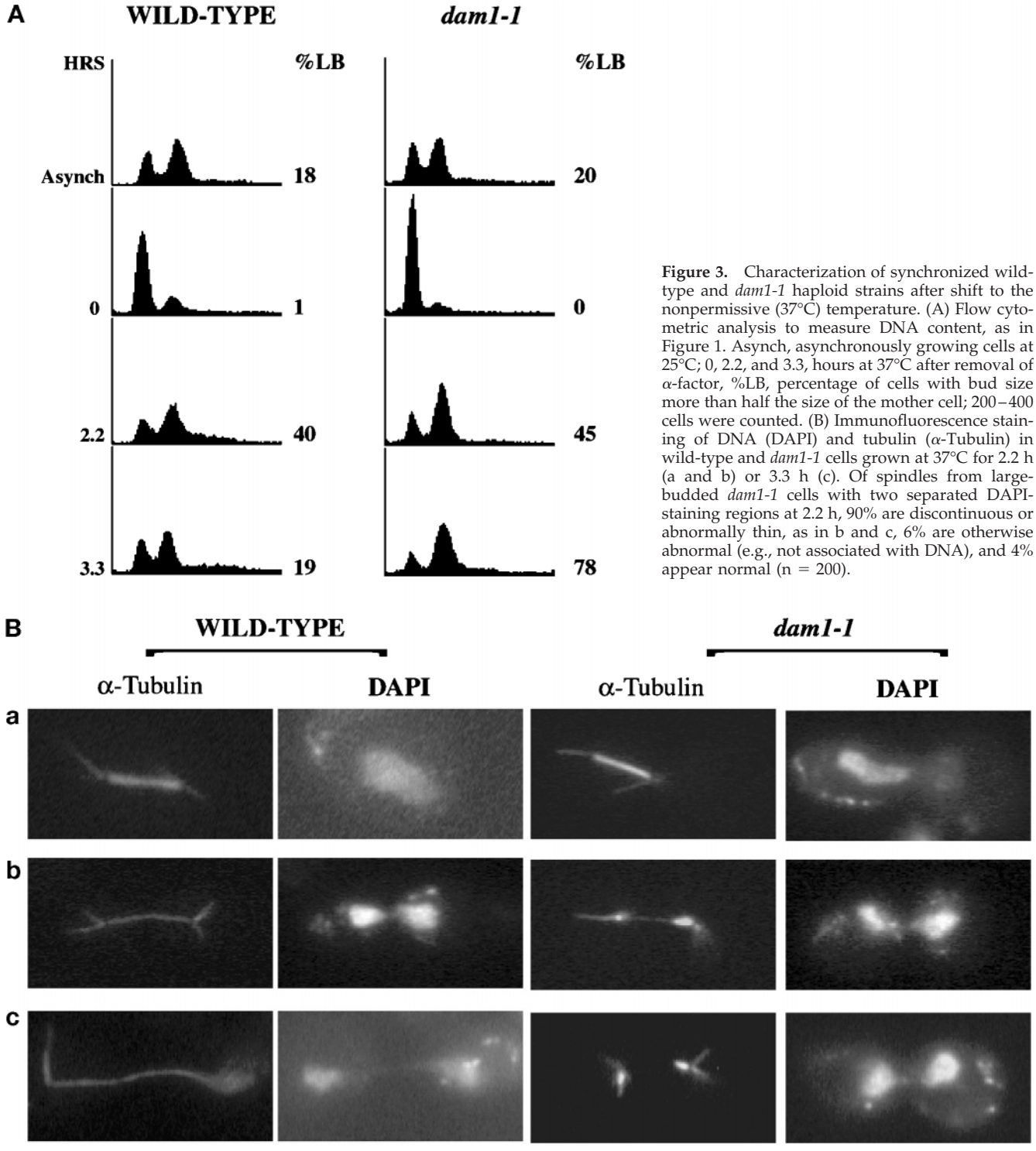

Figure 3. Characterization of synchronized wild-type and *dam1-1* haploid strains after shift to the nonpermissive (37°C) temperature. (A) Flow cytometric analysis to measure DNA content, as in Figure 1. Asynch, asynchronously growing cells at 25°C; 0, 2.2, and 3.3, hours at 37°C after removal of α-factor, %LB, percentage of cells with bud size more than half the size of the mother cell; 200–400 cells were counted. (B) Immunofluorescence staining of DNA (DAPI) and tubulin (α-Tubulin) in wild-type and *dam1-1* cells grown at 37°C for 2.2 h (a and b) or 3.3 h (c). Of spindles from large-budded *dam1-1* cells with two separated DAPI-staining regions at 2.2 h, 90% are discontinuous or abnormally thin, as in b and c, 6% are otherwise abnormal (e.g., not associated with DNA), and 4% appear normal (n = 200).

nonessential checkpoint role of Mps1p is essential in a *dam1-1* strain. A constitutive checkpoint requirement has been postulated for the spindle defect caused by a deletion of the *CIN8* gene, because mutation in all but one of the seven checkpoint genes causes lethality in this mutant strain (a lesser effect was seen in the *MAD3*Δ strain; Geiser *et al.*, 1997). Although *mps1-1* strains do not show a checkpoint defect at the permis-

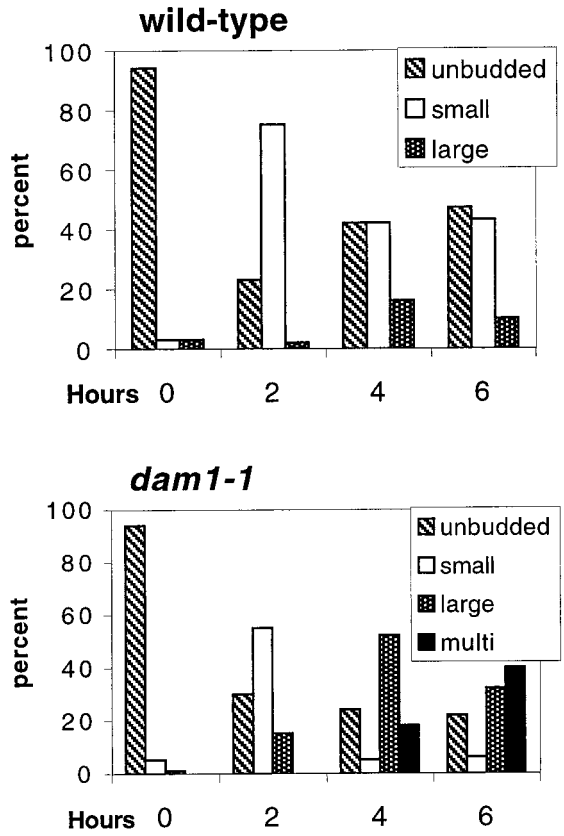

Figure 4. Budding indices of wild-type and *dam1-1* cells after release from α-factor arrest to the nonpermissive temperature represented as a bar graph. Each sample represents 200–400 cells examined.

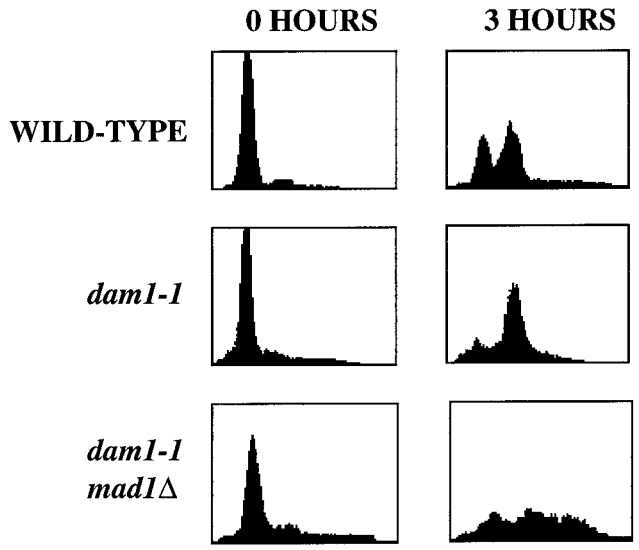

Figure 5. DNA content of wild-type, *dam1-1*, and *dam1-1mad1null* cells. Left panels (0 h), flow cytometric data of cells at α-factor arrest; right panels (3 h), flow cytometric data (performed as in Figures 1 and 3) of cells 3 h after release from α-factor to the nonpermissive temperature. Thirty-four percent (n = 400 cells) of *dam1-1, mad1*Δ cells were multibudded at this time point compared with 0% for both wild-type and *dam1-1* cells.

sive temperature (Weiss and Winey, 1996), it seems possible that even a slight checkpoint defect could be lethal in the presence of the *dam1-1* mutation. We tested this model by making double mutants between the *dam1-1* mutation and the *mad1, mad2*, and *mad3* null mutations (1325, 1491, and 1495; Table 1), each of which are defective in the spindle assembly checkpoint (Li and Murray, 1991). We found that these double mutant strains were viable with normal growth characteristics, indicating that *dam1-1* strains do not require the spindle assembly checkpoint for viability at the permissive temperature. Because *dam1-1* cells at the nonpermissive temperature do not display a short mitotic spindle with duplicated, unseparated DNA typical of cells arrested through the spindle assembly checkpoint pathway, it is possible that the mitotic bias observed in *dam1-1* cells is independent of this pathway. We tested this idea by comparing synchronized *dam1-1* and *dam1-1, mad1* null double mutant strains 3 h after release into the nonpermissive temperature (Figure 5). Although *dam1-1* cells show the previously described mitotic bias (Figure 5, *dam1-1*), this peak is missing in the cells lacking Mad1p (Figure 5, *dam1-1, mad1*Δ), suggesting that the defect caused by the *dam1-1* mutation at the nonpermissive temperature activates the spindle assembly checkpoint.

The dam1-1 Mutation Exhibits Genetic Interactions with Mutations in Other Spindle Proteins

The requirement for Dam1p in mitotic spindle function led us to determine whether the *dam1-1* mutation exhibits genetic interactions with mutations in other genes encoding proteins involved in mitosis, in addition to its genetic interaction with *MPS1*. No interactions were detected between the *dam1-1* mutation and alleles of genes encoding integral SPB components (*tub4-1*, *spc98-2*, and *cmd1-1*), kinetochore components (*ndc10-42* and *mif2-3*), or several proteins that act late in mitosis (*ase1*Δ and *mob1-77*) (our unpublished observations, mutations in genes encoding the mitotic spindle apparatus; for review, see Botstein *et al.*, 1997). Given the common occurrence of allele-specific interactions, these results clearly do not rule out the possibility of genetic interactions among different alleles of these genes. However, the *dam1-1* mutation was found to be lethal in combination with a deletion of either of the kinesin-like motor proteins encoded by *CIN8* or *KAR3* (but not with a deletion of *DYN1*) and to exacerbate *stu1-5*, a mutation in a microtubule-binding protein (Table 3). We examined dosage suppression of *dam1-1* with *STU1*, *KAR3*, and *CIN8* multicopy plasmids and of *stu1-5* and *cin8*Δ with a *DAM1* multicopy plasmid, but none was detected (our unpublished observation). Finally, we have observed

Table 3. Summary of synthetic interactions with *dam1-1*

Yeast strain	Relative growth			
	23°C	30°C	34°C	37°C
dam1-1	+	+	+	−
dam1-1, mps1-1	−	ND	ND	ND
*dam1-1, cin8*Δ	−	ND	ND	ND
*dam1-1, kar3*Δ	−	ND	ND	ND
stu1-5	+	+	+	±
dam1-1, stu1-5	+	±	−	−

+, size of colonies similar to a wild-type control; ±, size of colonies <20% of a wild-type control; −, no growth; ND, not determined.

that *dam1-1* strains are hypersensitive to growth on benomyl, a microtubule-destabilizing agent (our unpublished results). Genetic interactions between *DAM1* and genes that encode spindle components, together with the *dam1-1* phenotype and the in vitro microtubule-binding activity of Dam1p (Hofmann *et al.*, 1998), are consistent with a role of Dam1p in the function of the mitotic spindle. In addition, Stu1p has been shown to interact with Mps1p in 2-hybrid experiments (Luca and Winey, personal communication), and *CIN8* shows genetic interactions with *MPS1* (Geiser *et al.*, 1997), providing a further connection between *DAM1* and *MPS1*. The genetic interactions described here together with genetic and two hybrid interactions from the work of others (Hofmann *et al.*, 1998; Luca and Winey, personal communication) are summarized in Figure 6.

Dam1p Is Localized to the Spindle and Peripheral to the Spindle Pole

We investigated subcellular localization of the Dam1p protein at endogenous levels to determine whether the spindle defect observed in *dam1-1* mutant strains might be due to a direct role of Dam1p at the spindle. The chromosomal *DAM1* gene in a haploid strain was epitope tagged by integration of a triple c-*myc* epitope at its 3′ end (see MATERIALS AND METHODS). C-terminally *myc*-tagged Dam1p was detectable on Western blots (our unpublished observation), and the *myc-DAM1* strain (1345, Table 1) grows at a rate indistinguishable from wild-type strains at all temperatures checked (15–37°C), suggesting that the tagged *DAM1* allele is fully functional. Initial immunofluorescence experiments using an anti-*myc* antibody indicated that *myc*-Dam1p localizes with structures suggestive of spindle poles and short mitotic spindles (our unpublished observation). To verify this localization, the *myc-DAM1* allele was introduced into a strain containing an SPC42p–green fluorescent protein (GFP) fusion (Schutz and Winey, 1998) to visualize SPBs (1549; Table 1), or the *myc-DAM1* strain was doubly stained with both anti-*myc* and anti-tubulin (Tub1p) antibodies to visualize mitotic spindles. Using deconvolution microscopy on the *myc-DAM1, SPC42-GFP* strain (Figure 7), we observed *myc*-Dam1p localization immediately adjacent to SPBs when a single SPB was present (Figure 7a) and at a late stage in mitosis (Figure 7d). When the duplicated SPBs are still close together, *myc*-Dam1p clearly localizes between them (Figure 7b), presumably on the mitotic spindle, and starts to separate into two discrete foci as the SPBs move apart (Figure 7c). To quantitate this transition, we measured spindle lengths in a synchronized population of *myc-DAM1, SPC42-GFP* cells (1547; Table 1). *Myc*-Dam1p is present in a continuous bar of length 1.1–2.0 μm between SPBs (Figure 8, GROUP 1) and begins to separate into two discrete foci when the distance is ≥1.9 μm (Figure 8, GROUP 2). The spindle localization was confirmed in the *myc-DAM1* strain (1345; Table 1) by immunofluorescence experiments using α-*myc* and α-Tub1p antibodies (Figure 9). Through the short spindle stage (Figure 9A, a–c), *myc*-Dam1p colocalizes with tubulin and generally reflects microtubule density. At later stages in mitosis, *myc*-Dam1p staining appears more strongly at the spindle poles (Figure 9A, d and e) and does not appear to correlate with microtubule density. In this experiment, we also were able to detect punctate nuclear *myc*-Dam1p staining throughout the cell cycle by using a more sensitive FITC-conjugated secondary antibody to the α-*myc* antibody (not possible with the *SPC42-GFP* strain). Treatment with the microtubule-destabilizing drugs nocodozole and benomyl abolishes the majority of microtubule and *myc*-Dam1p staining (Figure 9B, left panel, right cell), although we observed the punctate nuclear staining in the absence of microtubules (Figure 9B, right panel). In cells with residual microtubule staining, there remains proportionally reduced *myc*-Dam1p staining as well (Figure 9B, left panel, left cell).

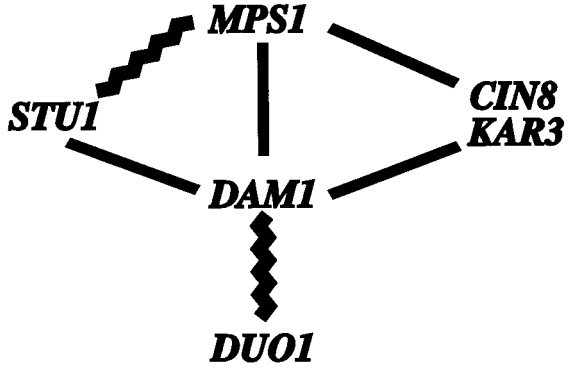

Figure 6. Summary of genetic and two-hybrid interactions involving *DAM1*. Jagged lines denote two-hybrid interactions, and straight lines denote synthetic lethal interactions. The *CIN8-MPS1* data are from Geiser *et al.* (1997). The *STU1-MPS1* data are from Luca and Winey (personal communication). The *DAM1-DUO1* data are from Hofman *et al*. (1998).

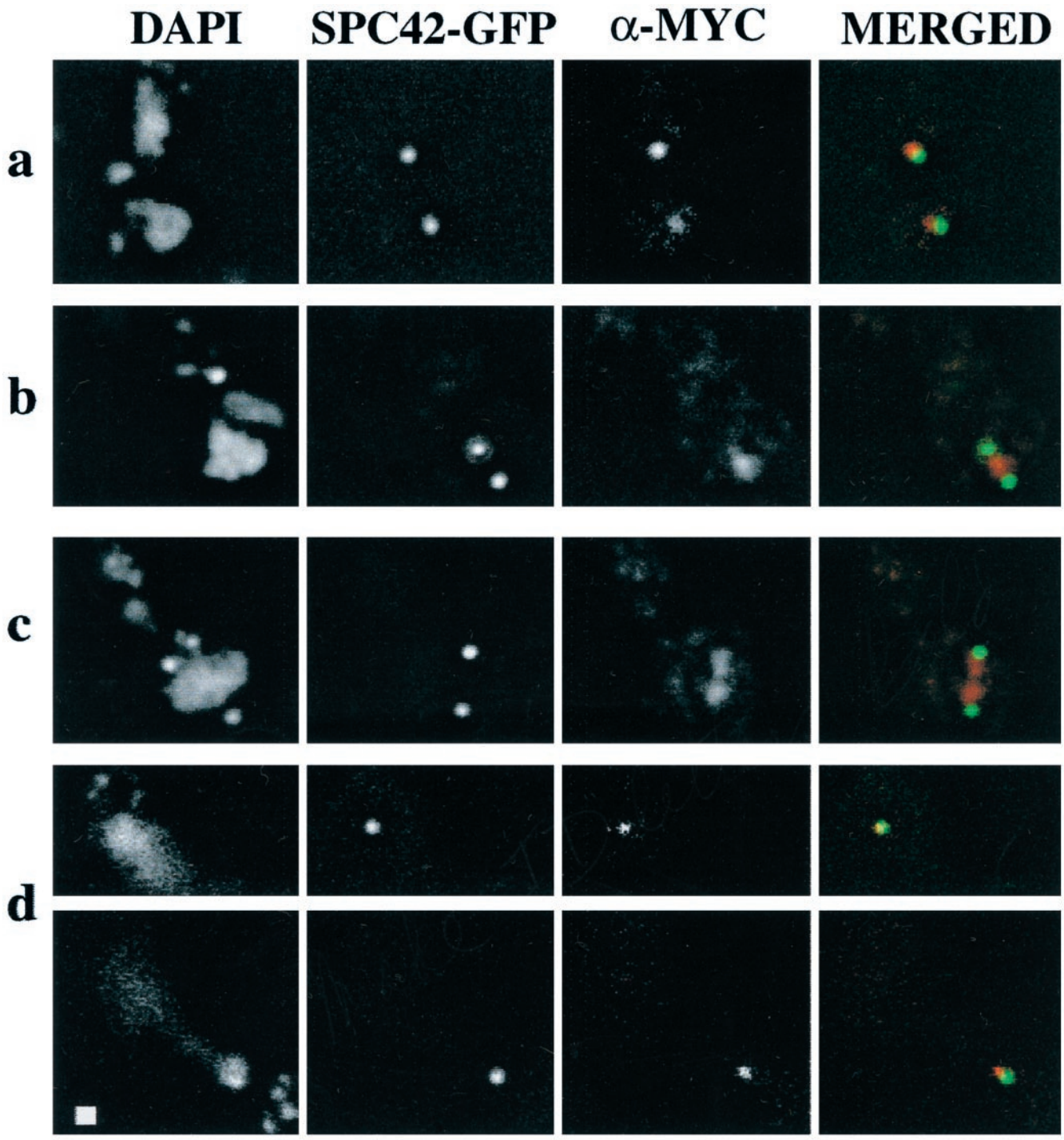

Figure 7. Localization of *myc*-Dam1p in wild-type yeast cells using immunofluorescence microscopy. DAPI, DNA staining; SPC42-GFP, autofluorescence of a GFP-tagged version of Spc42p; α-MYC, anti-*myc* 1° antibody plus Texas Red anti-mouse 2° antibody; MERGED, merging of fluorescence of SPC42-GFP (green) and α-MYC (red). (a) Two unbudded cells. (b and c) Budded cells with short spindles before anaphase B elongation. (d) Two focal planes of a large budded cell in late anaphase. Bar, 1 μm.

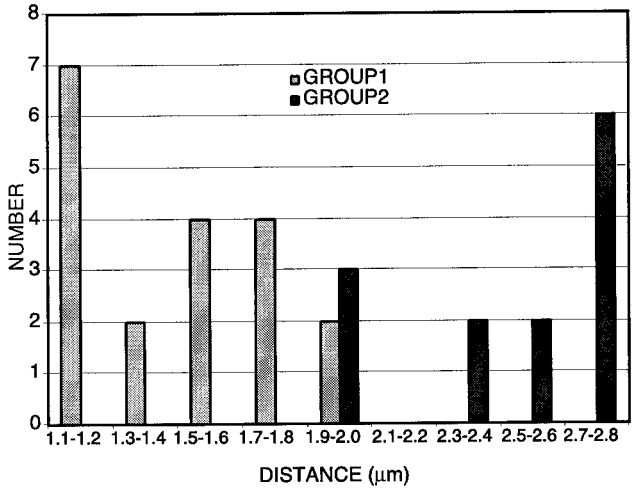

Figure 8. Transition of *myc*-Dam1p localization from one to two foci. Bar graph of spindle lengths in cells with the following patterns of *myc*-Dam1p staining. GROUP 1, *myc*-Dam1p localization as an uninterrupted bar between the SPBs (n = 19; average = 1.5 μm; SD = 0.3); GROUP 2, *myc*-Dam1p localization as two staining regions adjacent to the SPBs (n = 13; average = 2.4 μm; SD = 0.3). Spindles were measured using Slidebook software with an error of ±0.1 μm.

DISCUSSION

We have reported the isolation of mutations in three distinct classes of genes that are synthetically lethal with the *mps1-1* mutation. The first includes genes that encode the molecular chaperones *CDC37, YDJ1, HSC82,* and *STI1*. The second class is defined by *BUB1*, a gene required for the spindle assembly checkpoint. The final class contains the *DAM1* gene that encodes an essential spindle- and spindle pole-localized protein required for mitotic spindle function.

We previously demonstrated that Mps1p activity requires the Cdc37p chaperone (Schutz *et al.*, 1997). In this study, we isolated both conditional and nonconditional alleles of *CDC37* that are lethal in combination with the *mps1-1* mutation. Cells containing the conditional allele of *CDC37* arrest in G1 with unreplicated DNA at the nonpermissive temperature as do the previously characterized alleles of this gene (Schutz *et al.*, 1997; Schutz, Ph.D. thesis). In addition to *CDC37*, we found that *mps1-1* strains require wild-type activity of *YDJ1*, *HSC82*, and *STI1* for their viability. As mentioned previously, the *HSC82*-encoded Hsp90p and Sti1p are found in a macromolecular chaperone complex, and Ydj1p interacts with and regulates Sti1p (Cyr *et al.*, 1992; Cyr and Douglas, 1994; Cyr, 1995). Mutations in members of this chaperone complex and in *CDC37* have been identified in synthetic lethal screens with other defective kinases, including *kin28-ts3* and *cdc28-109* (Valay *et al.*, 1995; Zarzov *et al.*, 1997). It is possible that this group of chaperones functions to stabilize the compromised kinases at their normally permissive temperatures. Similar to alleles of *CDC37,* strains harboring mutant alleles of other chaperones also exhibit SPB defects. Cell harboring either *ydj1-10* or *hsf1-82*, which is defective in the synthesis of Hsp90p, have been found to arrest with large buds and a single focus of microtubules at restrictive temperatures. Electron microscopic analysis of *hsf1-82* cells revealed an unduplicated SPB with an enlarged half-bridge, reminiscent of the *mps1-1* SPB defect (Zarzov *et al.*, 1997). Our results suggest that this phenotype may be due to instability of Mps1p caused by decreased Hsp90p in the cell. Although growth in *sti1* null mutants is compromised at restrictive temperatures, detailed cytology of these mutants is not yet available (Nicolet and Craig, 1989). Based on the different terminal SPB phenotypes in *cdc37-1* and *ydj1-10* and *hsf1-82* mutants, it is likely that these genes affect different steps in Mps1p activation or define more than one requirement for chaperones to activate or maintain Mps1p kinase activity and possibly the activity of other kinases.

In addition to requiring molecular chaperones, the *mps1-1* mutation shows synthetic lethality with a checkpoint-defective allele of the gene encoding the Bub1p protein kinase (Roberts *et al.*, 1994). Interestingly, *mps1-1* is viable in combination with other mutations in the checkpoint pathway (Hardwick *et al.* 1996), suggesting that the synthetic lethality is not due to a requirement for other checkpoint proteins in general but instead that a closer link may exist between *MPS1* and *BUB1* than previously suspected. *MPS1* and *BUB1* (and *BUB3*, whose product forms a complex with Bub1p; Roberts *et al.*, 1994) are distinct from other checkpoint genes in that null mutations in them have drastic effects on cell viability indicative of other roles in the cell in addition to their nonessential checkpoint functions (Roberts *et al.*, 1994). Also, mutations in both *MPS1* and *BUB1* have been found to be synthetically lethal with a deletion allele of the *CIN8* kinesin-like motor (Geiser *et al.*, 1997). Regardless of the molecular nature of this interaction, it is interesting that these two kinases appear to interact in some way beyond their role in the spindle assembly checkpoint.

The third class of genes reported here is represented by *DAM1*. Dam1p shows no homology to other genes in *S. cerevisiae* or in other organisms, but it does contain coiled coil domains as defined by the COILS program (Lupas *et al.*, 1991; our unpublished observation), often seen in structural proteins. *DAM1* was independently identified in a two-hybrid screen with the *DUO1* gene, and Dam1p has been shown to bind microtubules in vitro (Hofmann *et al.*, 1998). Furthermore, overexpression of *DAM1* (and *DUO1*) results in spindle defects. Consistent with these data, we report that Dam1p is required for the integrity of the spindle during anaphase B elongation. However, we uncovered *DAM1* using a very different approach, in an *mps1-1*-based screen designed to detail interactions

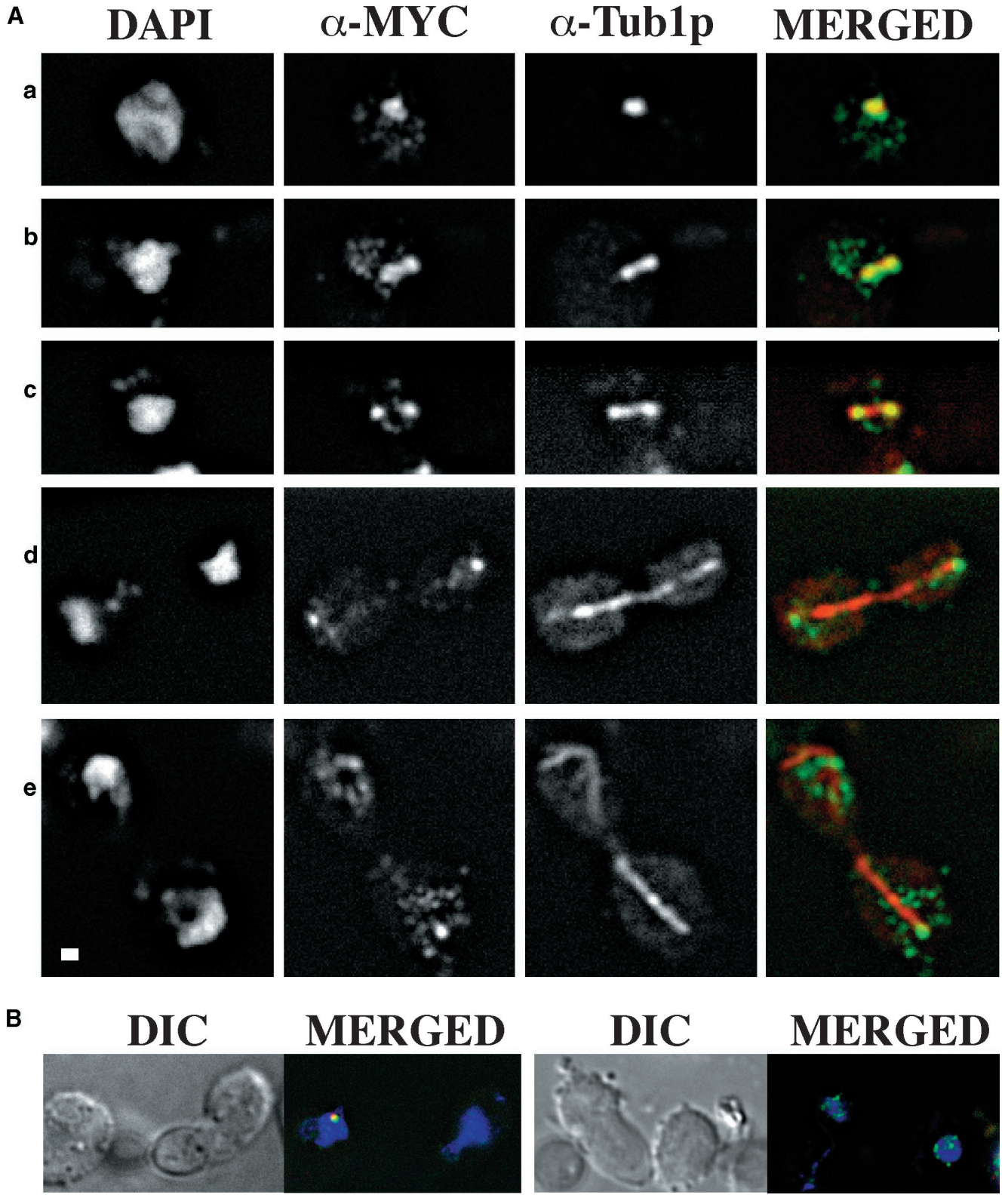

Figure 9.

necessary for SPB duplication and the spindle assembly checkpoint functions. We eliminated the possibility that the *dam1-1* defect at the permissive temperature leads to a constitutive requirement for the checkpoint pathway by demonstrating viability of double mutants containing *dam1-1* and a null allele of one of several other checkpoint-related genes. At the nonpermissive temperature, *dam1-1* cells do appear to be defective in maintenance of a checkpoint arrest state; however, activation of the checkpoint, the step in which Mps1p acts, appears to be intact (Figure 5).

Therefore, the interaction between *MPS1* and *DAM1* is probably through the role of Mps1p in SPB duplication or through an as yet uncharacterized role in spindle dynamics. The latter role has been suggested by a demonstrated physical interaction between Mps1p and Stu1p (Luca and Winey, personal communication); Stu1p is a spindle and spindle pole component that was identified originally as an extragenic suppressor of a mutation in the β-tubulin-encoding gene *TUB2* (Pasqualone and Huffaker, 1994). In addition, two nonconditional alleles of *MPS1* have been shown to be synthetically lethal with a deletion of *CIN8* (Geiser *et al.*, 1997), a gene encoding a kinesin-like motor protein involved in spindle assembly and maintenance (Hoyt *et al.*, 1992; Roof *et al.*, 1992; Saunders *et al.*, 1995), and in the "rapid" phase (Straight *et al.*, 1998) of anaphase B chromosome separation (Saunders *et al.*, 1997). We have shown genetic interactions between the *dam1-1* mutation and mutations in the *CIN8*, *KAR3*, and *STU1* genes (Figure 6) and favor the idea that *DAM1* interacts with *MPS1* through spindle functions after SPB duplication in the cell cycle. This idea will be tested with the isolation of *mps1* mutations specific to one of its several roles. Also, further studies involving localization of Dam1p in the *mps1-1* mutant strain may shed light on the molecular basis of the *dam1-1, mps1-1* synthetic lethality. We do not observe a physical interaction between Mps1p and Dam1p using two-hybrid or coimmunoprecipitation assays (our unpublished observation), suggesting that if a physical association exists between these two proteins, it is likely to be transient or limited to the context of the spindle and spindle pole. It will also be interesting to test whether Dam1p is phosphorylated, because the genetic interaction may be indicative of a kinase–substrate relationship.

We have shown that an epitope-tagged version of Dam1p at endogenous levels exhibits an interesting pattern of localization during the cell cycle, associating with short spindles initially and moving to spindle poles as spindles elongate during mitosis. The presence of Dam1p at the spindle pole is likely mediated through its microtubule-binding activity (Hofmann *et al.*, 1998); this idea is consistent with the dramatic decrease in staining upon depolymerization of microtubules and genetic interactions observed between *DAM1* and genes encoding spindle components, such as Stu1p, Cin8p, and Kar3p. The pattern we observe is a subset of that seen upon overexpression of the protein in which it appears to bind the entire spindle and spindle poles at all times during the cell cycle (Hofmann *et al.*, 1998). One explanation for this difference is that increasing the amount of protein drives its association with the spindle, eventually leading to the observed toxicity for the cell. Interestingly, Duo1p, a binding partner of Dam1p, is found on spindles and spindle poles at endogenous levels throughout the cell cycle (Hofmann *et al.*, 1998).

Mitotic spindles contain two general classes of microtubules that can be defined functionally and morphologically (Winey *et al.*, 1995; Straight *et al.*, 1997). One class of microtubules interdigitate in the spindle midzone to define a core bundle that lengthen during anaphase spindle elongation. Some microtubule-associated proteins in yeast, such as Ase1p, appear to be localized to this group of spindle microtubules (Pellman *et al.*, 1995). The other class of spindle microtubules makes up the kinetochore fibers. In budding yeast, a kinetochore fiber is comprised of a single microtubule joining the SPB to a chromosome (Peterson and Ris, 1976; Winey *et al.*, 1995). There are no reported proteins that bind specifically to kinetochore microtubules. Thus far, it is not clear whether Dam1p is specifically associated with one or both of these types of microtubules. The terminal broken spindle phenotype in *dam1-1* strains occurs during anaphase B elongation, consistent with a potential role for Dam1p in stabilizing the region of overlap in the spindle midzone, i.e., in the first class of microtubles. However, the redistribution of the wild-type Dam1p from entire spindle to spindle pole during mitotic progression is more reminiscent of the dynamics of kinetochore movement, and a similar pattern of localization is seen with the kinetochore proteins Ndc10p (Goh and Kilmartin, 1993), Ndc80p (Wigge *et al.*, 1998), and Cse4p (Meluh *et al.*, 1998). The SPB-proximal staining is similar to kinetochore proteins Ctf19p (Hyland *et al.*, 1999) and Mif2p (Meluh and Koshland, 1997). Kinetochore fibers occupy a significant amount of space in short spindles but early in mitosis diminish in length until very short remnants remain at the spindle poles during later stages of mitosis (Winey *et al.*, 1995). In fact,

Figure 9 (facing page). Colocalization of *myc*-Dam1p with microtubules using immunofluorescence microscopy. (A) DAPI, DNA staining; α-MYC, anti-*myc* 1° antibody plus FITC anti-mouse 2° antibody; α-Tub1-GFP, anti-tubulin 1° antibody plus Texas Red anti-rat 2° antibody. The granular staining using Texas Red is present in controls lacking primary antibody and is considered background. MERGED, merging of α-MYC (green) and α-Tub1p fluorescence (red). (a) Unbudded cell. (b and c) Budded cells with short spindles before anaphase B elongation. (d and e) Large budded cells in late anaphase. (B) *myc*-Dam1p localization after treatment of cells with microtubule-depolymerizing agents. DIC (differential interference contrast) shows cell outline. MERGED, merging of DAPI (blue), α-MYC (green), and α-Tub1p (red) fluorescence. The left panel shows residual colocalization (yellow) of *myc*-Dam1p (green) and tubulin (red), and the right panel shows punctate nuclear *myc*-Dam1p staining (green) in the absence of microtubules (red). Bar, 1 μm.

the reduction during anaphase A in kinetochore microtubule number and length as documented by electron microscopy (Winey *et al*., 1995) occurs in spindles of ~2 μm in length, showing good correlation with the spindle length in which we observe Dam1p concentrating at the poles. In addition, the unusual discontinuous spindle phenotype observed in the *dam1-1* mutant strain resembles, at least superficially, that described for a mutation in *MIF2* (Brown *et al*., 1993). However, we have not detected any genetic interactions between *DAM1* and *NDC10* or *MIF2*. Although it is difficult to envision how a kinetochore microtubule-binding protein could affect anaphase elongation, one possibility is that *dam1-1* could cause a defect in spindle structure, resulting in a tension imbalance in the spindle that is manifested as a broken spindle phenotype.

A higher-resolution analysis of the Dam1p localization will be necessary to reveal its exact location in mitotic spindles. In addition, further analysis of Dam1p will be necessary to understand the basis of the genetic interaction between the *dam1-1* and *mps1-1* mutations. This analysis should yield a clearer understanding of the function of this novel microtubule-binding spindle protein.

ACKNOWLEDGMENTS

We thank D. Drubin, G. Barnes, and I. Cheeseman for communicating results before publication, M. Brown, C. Connelly, P. Heiter, T. Davis, M. Hoyt, K. Hardwick, T. Huffaker, J. Kilmartin, F. Luca, P. Meluh, D. Pellman, E. Schiebel, and A. Straight for reagents, L. Pillus, T. Su, C. Troxel, and J. Yucel for critical reading of the manuscript, our reviewers for several helpful insights, and members of the Winey and Drubin–Barnes laboratories for helpful discussion. This work was supported by fellowships from the National Institutes of Health (GM-19566 to A.R.C.) and the Cancer League of Colorado (to J.B.B.) and by grants from the National Institutes of Health (GM-51312) and the National Science Foundation (MCB-09357033). Deconvolution microscopy was made possible, in part, by a gift from Virginia and Mel Clark.

REFERENCES

Baudin, A., Ozier-Kalogeropoulos, O., Denouel, A., Lacroute, F., and Cullin, C. (1993). A simple and efficient method for direct gene deletion in *Saccharomyces cerevisiae.* Nucleic Acids Res. *21*, 3329–3330.

Bender, A., and Pringle, J.R. (1991). Use of a screen for synthetic lethal and multicopy suppresser mutants to identify two new genes involved in morphogenesis in *Saccharomyces cerevisiae.* Mol. Cell. Biol. *11*, 1295–1305.

Boeke, J.D., Trueheart, J., Natsoulis, G., and Fink, G.R. (1987). 5-Fluoroorotic acid as a selective agent in yeast molecular genetics. Methods Enzymol. *154*, 164–175.

Botstein, D., Amberg, D., Mulholland, J., Huffaker, T., Adams, A., Drubin, D., and Stearns, T. (1997). The yeast cytoskeleton. In: The Molecular and Cellular Biology of the Yeast *Saccharomyces*: Cell Cycle and Cell Biology, ed. J.R. Pringle, J.R. Broach, and E.W. Jones, Cold Spring Harbor, NY: Cold Spring Harbor Laboratory Press, 1–90.

Brown, M.T., Goetsch, L., and Hartwell, L.H. (1993). *MIF2* is required for mitotic spindle integrity during anaphase spindle elongation in *Saccharomyces cerevisiae.* J. Cell Biol. *123*, 387–403.

Byers, B., and Goetsch, L. (1974). Duplication of spindle plaques and integration of the yeast cell cycle. Cold Spring Harb. Symp. Quant. Biol. *38*, 123–131.

Byers, B., and Goetsch, L. (1975). Behavior of spindles and spindle plaques in the cell cycle and conjugation of *Saccharomyces cerevisiae.* J. Bacteriol. *124*, 511–523.

Byers, B., and Goetsch, L. (1991). Preparation of yeast cells for thin-section electron microscopy. Methods Enzymol. *194*, 602–608.

Chang, H.C., and Lindquist, S. (1994). Conservation of Hsp90 macromolecular complexes in *Saccharomyces cerevisiae.* J. Biol. Chem. *269*, 24983–24988.

Chial, H.J., Rout, M.P., Giddings, T.H., Jr., and Winey, M. (1998). *Saccharomyces cerevisiae* Ndc1p is a shared component of nuclear pore complexes and spindle pole bodies. J. Cell Biol. *143*, 1789–1800.

Cohen-Fix, O., Peters, J.M., Kirschner, M.W., and Koshland, D. (1996). Anaphase initiation in *Saccharomyces cerevisiae* is controlled by the APC-dependent degradation of the anaphase inhibitor Pds1p. Genes & Dev. *10*, 3081–3093.

Cyr, D.M. (1995). Cooperation of the molecular chaperone Ydj1 with specific Hsp70 homologs to suppress protein aggregation. FEBS Lett. *359*, 129–132.

Cyr, D.M., and Douglas, M.G. (1994). Differential regulation of Hsp70 subfamilies by the eukaryotic DnaJ homologue YDJ1. J. Biol. Chem. *269*, 9798–9804.

Cyr, D.M., Lu, X., and Douglas, M.G. (1992). Regulation of Hsp70 function by a eukaryotic DnaJ homolog. J. Biol. Chem. *267*, 20927–20931.

Elledge, S.J. (1996). Cell cycle checkpoints: preventing an identity crisis. Science *274*, 1664–1672.

Geiser, J.R., Schott, E.J., Kingsbury, T.J., Cole, N.B., Totis, L.J., Bhattacharyya, G., He, L., and Hoyt, M.A. (1997). *Saccharomyces cerevisiae* genes required in the absence of the *CIN8*-encoded spindle motor act in functionally diverse mitotic pathways. Mol. Biol. Cell *8*, 1035–1050.

Goh, P.Y., and Kilmartin, J.V. (1993). *NDC10*: a gene involved in chromosome segregation in *Saccharomyces cerevisiae.* J. Cell Biol. *121*, 503–512.

Guthrie, C., and Fink, G.R. (1991). Guide to Yeast Genetics and Molecular Biology, vol. 194. Methods in Enzymology, San Diego: Academic Press.

Hardwick, K.G., Weiss, E., Luca, F.C., Winey, M., and Murray, A.W. (1996). Activation of the budding yeast spindle assembly checkpoint without mitotic spindle disruption. Science *273*, 953–956.

Hofmann, C., Cheeseman, I.M., Goode, B.L., McDonald, K.L., Barnes, G., and Drubin, D.G. (1998). *Saccharomyces cerevisiae* Duo1p and Dam1p, novel proteins involved in mitotic spindle function. J. Cell Biol. *143*, 1029–1040.

Hoyt, M.A., and Geiser, J.R. (1996). Genetic analysis of the mitotic spindle. Annu Rev. Genet. *30*, 7–33.

Hoyt, M.A., He, L., Loo, K.K., and Saunders, W.S. (1992). Two *Saccharomyces cerevisiae* kinesin-related gene products required for mitotic spindle assembly. J. Cell Biol. *118*, 109–120.

Hoyt, M.A., Totis, L., and Roberts, B.T. (1991). *S. cerevisiae* genes required for cell cycle arrest in response to loss of microtubule function. Cell *66*, 507–517.

Hutter, K.J., and Eipel, H.E. (1979). Microbial determinations by flow cytometry. J. Gen. Microbiol. *113*, 369–375.

Hyland, K.M., Kingsbury, J., Koshland, D., and Hieter, P. (1999). Ctf19p: a novel kinetochore protein *Saccharomyces cerevisiae* and a potential link between the kinetochore and mitotic spindle. J. Cell Biol. *145*, 15–28.

Jakob, U., and Buchner, J. (1994). Assisting spontaneity: the role of Hsp90 and small Hsps as molecular chaperones. Trends Biochem. Sci. *19*, 205–211.

Juang, Y.L., Huang, J., Peters, J.M., McLaughlin, M.E., Tai, C.Y., and Pellman, D. (1997). APC-mediated proteolysis of Ase1 and the morphogenesis of the mitotic spindle. Science *275*, 1311–1314.

Kellogg, D.R., Moritz, M., and Alberts, B.M. (1994). The centrosome and cellular organization. Annu. Rev. Biochem. *63*, 639–674.

Knop, M., Pereira, G., Geissler, S., Grein, K., and Schiebel, E. (1997). The spindle pole body component Spc97p interacts with the gamma-tubulin of *Saccharomyces cerevisiae* and functions in microtubule organization and spindle pole body duplication. EMBO J. *16*, 1550–1564.

Knop, M., and Schiebel, E. (1997). Spc98p and Spc97p of the yeast gamma-tubulin complex mediate binding to the spindle pole body via their interaction with Spc110p. EMBO J. *16*, 6985–6995.

Knop, M., and Schiebel, E. (1998). Receptors determine the cellular localization of a gamma-tubulin complex and thereby the site of microtubule formation. EMBO J. *17*, 3952–3967.

Kolodziej, P.A., and Young, R.A. (1991). Epitope tagging and protein surveillance. Methods Enzymol. *194*, 508–519.

Lauze, E., Stoelcker, B., Luca, F.C., Weiss, E., Schutz, A.R., and Winey, M. (1995). Yeast spindle pole body duplication gene *MPS1* encodes an essential dual specificity protein kinase. EMBO J. *14*, 1655–1663.

Li, R., and Murray A.W. (1991). Feedback control of mitosis in budding yeast. Cell *66*, 519–531.

Luca, F.C., and Winey, M. (1998). *MOB1*, an essential yeast gene required for completion of mitosis and maintenance of ploidy. Mol. Biol. Cell *9*, 29–46.

Lupas, A., Van Dyke, M., and Stock, J. (1991). Predicting coiled coils from protein sequences. Science *252*, 1162–1164.

Meluh, P.B., and Koshland, D. (1997). Budding yeast centromere composition and assembly as revealed by in vivo cross-linking. Genes & Dev *11*, 3401–3412.

Meluh, P.B., Yang, P., Glowczewski, L., Koshland, D., and Smith, M.M. (1998). Cse4p is a component of the core centromere of *Saccharomyces cerevisiae*. Cell *94*, 607–613.

Nathan, D.F., and Lindquist, S. (1995). Mutational analysis of Hsp90 function: interactions with a steroid receptor and a protein kinase. Mol. Cell. Biol. *15*, 3917–3925.

Nicolet, C.M., and Craig, E.A. (1989). Isolation and characterization of *STI1*, a stress-inducible gene from *Saccharomyces cerevisiae*. Mol. Cell. Biol. *9*, 3638–3646.

Pasqualone, D., and Huffaker, T.C. (1994). *STU1*, a suppressor of a beta-tubulin mutation, encodes a novel and essential component of the yeast mitotic spindle. J. Cell Biol. *127*, 1973–1984.

Pellman, D., Bagget, M., Tu, Y.H., Fink, G.R., and Tu, H. (1995). Two microtubule-associated proteins required for anaphase spindle movement in *Saccharomyces cerevisiae*. J. Cell Biol. *130*, 1373–1385.

Peterson, J.B., and Ris, H. (1976). Electron-microscopic study of the spindle and chromosome movement in the yeast *Saccharomyces cerevisiae*. J. Cell Sci. *22*, 219–242.

Pratt, W.B. (1992). Control of steroid receptor function and cytoplasmic-nuclear transport by heat shock proteins. Bioessays *14*, 841–848.

Pringle, J.R., Adams, A.E., Drubin, D.G., and Haarer, B.K. (1991). Immunofluorescence methods for yeast. Methods Enzymol. *194*, 565–602.

Roberts, B.T., Farr, K.A., and Hoyt, M.A. (1994). The *Saccharomyces cerevisiae* checkpoint gene *BUB1* encodes a novel protein kinase. Mol. Cell. Biol. *14*, 8282–8291.

Roof, D.M., Meluh, P.B., and Rose, M.D. (1992). Kinesin-related proteins required for assembly of the mitotic spindle. J. Cell Biol. *118*, 95–108.

Rudner, A.D., and Murray, A.W. (1996). The spindle assembly checkpoint. Curr. Opin. Cell Biol. *8*, 773–780.

Saunders, W., Lengyel, V., and Hoyt, M.A. (1997). Mitotic spindle function in *Saccharomyces cerevisiae* requires a balance between different types of kinesin-related motors. Mol. Biol. Cell *8*, 1025–1033.

Saunders, W.S., Koshland, D., Eshel, D., Gibbons, I.R., and Hoyt, M.A. (1995). *Saccharomyces cerevisiae* kinesin- and dynein-related proteins required for anaphase chromosome segregation. J. Cell Biol. *128*, 617–624.

Schutz, A.R. (1997). *MPS1* and *CDC37*: Analysis of Two Genes Required for Spindle Pole Body Duplication in Budding Yeast. Ph.D. Thesis. Boulder, CO: University of Colorado.

Schutz, A.R., Giddings, T.H., Jr., Steiner, E., and Winey. M. (1997). The yeast *CDC37* gene interacts with *MPS1* and is required for proper execution of spindle pole body duplication. J. Cell Biol. *136*, 969–982.

Schutz, A.R., and Winey, M. (1998). New alleles of the yeast *MPS1* gene reveal multiple requirements in spindle pole body duplication. Mol. Biol. Cell *9*, 759–774.

Sikorski, R.S., and Hieter, P. (1989). A system of shuttle vectors and yeast host strains designed for efficient manipulation of DNA in *Saccharomyces cerevisiae*. Genetics *122*, 19–27.

Straight, A.F., Marshall, W.F., Sedat, J.W., and Murray, A.W. (1997). Mitosis in living budding yeast: anaphase A but no metaphase plate. Science *277*, 574–578.

Straight, A.F., Sedat, J.W., and Murray, A.W. (1998). Time-lapse microscopy reveals unique roles for kinesins during anaphase in budding yeast. J. Cell Biol. *143*, 687–694.

Sundberg, H.A., and Davis, T.N. (1997). A mutational analysis identifies three functional regions of the spindle pole component Spc110p in *Saccharomyces cerevisiae*. Mol. Biol. Cell *8*, 2575–2590.

Valay, J.G., Simon, M., Dubois, M.F., Bensaude, O., Facca, C., and Faye, C. (1995). The *KIN28* gene is required both for RNA polymerase II mediated transcription and phosphorylation of the Rpb1p CTD. J. Mol. Biol. *249*, 535–544.

Weiss, E., and Winey, M. (1996). The *Saccharomyces cerevisiae* spindle pole body duplication gene *MPS1* is part of a mitotic checkpoint. J. Cell Biol. *132*, 111–123.

Wells, W.A., and Murray, A.W. (1996). Aberrantly segregating centromeres activate the spindle assembly checkpoint in budding yeast. J. Cell Biol. *133*, 75–84.

Wigge, P.A., Jensen, O.N., Holmes, S., Soues, S., Mann, M., and Kilmartin, J.V. (1998). Analysis of the *Saccharomyces* spindle pole by matrix-assisted laser desorption/ionization (MALDI) mass spectrometry. J. Cell Biol. *141*, 967–977.

Winey, M., and Byers, B. (1993). Assembly and functions of the spindle pole body in budding yeast. Trends Genet. *9*, 300–304.

Winey, M., Goetsch, L., Baum, P., and Byers, B. (1991). *MPS1* and *MPS2*: novel yeast genes defining distinct steps of spindle pole body duplication. J. Cell Biol. *114*, 745–754.

Winey, M., Mamay, C.L., O'Toole, E.T., Mastronarde, D.N., Giddings, T.H., Jr., McDonald, K.L., and McIntosh, J.R. (1995). Three-dimensional ultrastructural analysis of the *Saccharomyces cerevisiae* mitotic spindle. J. Cell Biol. *129*, 1601–1615.

Winsor, B., and Schiebel, E. (1997). Review: an overview of the *Saccharomyces cerevisiae* microtubule and microfilament cytoskeleton. Yeast *13*, 399–434.

Zarzov, P., Boucherie, H., and Mann, C. (1997). A yeast heat shock transcription factor (Hsf1) mutant is defective in both Hsc82/Hsp82 synthesis and spindle pole body duplication. J. Cell Sci. *110*, 1879–1891.